

# Performance constraints on the MCS super-resolution algorithm

Michael P. Egan

*National Geospatial-Intelligence Agency  
Basic and Applied Research Office*

## ABSTRACT

In previous work we have demonstrated the ability of the algorithm developed by Magain, Courbin, and Sohy (MCS, ApJ 2008 [1]) to resolve point sources and filamentary extended sources that have positions closer than the traditional  $1.22\lambda/D$  diffraction limit of an optical system. The efficacy of the technique depends on a number of factors, including the signal-to-noise-ratio (SNR), the ‘blackness’ of the overall image, knowledge of the original system point response function, etc. In this paper we explore the effect of these parameters on the results of the algorithm to determine the point at which the positions and amplitudes of sources reconstructed using the MCS algorithm become unreliable.

## 1. INTRODUCTION

In a previous papers Egan ([2], [3]) examined the MCS method for super-resolution reconstruction of astronomical imaging as applied to data from the Midcourse Space Experiment (MSX) and to simulated filamentary data. The MCS method seeks a higher resolution model of data by minimizing a function consisting of a data integrity term and a regularization term in the form

$$S = \sum_{i=1}^N \frac{1}{\sigma_i^2} \left[ \sum_{j=1}^N t_{ij} f_j - d_i \right]^2 + \lambda H(\mathbf{f})$$

where the first term is the data integrity term which is a  $\chi^2$  term quantifying the uncertainty weighted difference between the modeled true image,  $\mathbf{t} \otimes \mathbf{f}$  and the measured data,  $\mathbf{d}$ . In this formulation,  $\mathbf{f}$  is the super-resolved image, which is convolved with a kernel  $\mathbf{t}$  that blurs the super-resolved image to the inferior resolution of the measured data. Discussion of the details of the method and its numerical solution can be found in [1], [2], and [3].

The MCS algorithm is based on the principle that sampled data cannot be fully deconvolved, i.e. yielding delta function-type point sources, without violating the sampling theorem. In detail, the MCS technique minimizes the function

$$S_2 = \sum \frac{1}{\sigma^2} \left[ \mathbf{s} \otimes \left( \mathbf{h} + \sum_{k=1}^M a_k \mathbf{r}(\mathbf{x} - c_k) \right) - \mathbf{d} \right]^2 + \lambda \sum (\mathbf{h} - \mathbf{r} \otimes \mathbf{h})^2$$

where the point response function (PRF) of the original imaging system is represented by

$$\mathbf{p} = \mathbf{r} \otimes \mathbf{s}.$$

In the above equation the original data PRF,  $\mathbf{p}$  is assumed to be reproducible by the convolution of the PRF of the ‘‘ideal’’ system,  $\mathbf{r}$ , and the ‘‘deconvolution kernel’’  $\mathbf{s}$ . The ‘‘ideal’’ system defines the resolution, and the image sampling needed for the super-resolution image. In practice, since  $\mathbf{p}$  is known, and  $\mathbf{r}$  is defined by the user, the deconvolution kernel,  $\mathbf{s}$  is solved for from these. Instead of a global technique, MCS opts for a regularization function that imposes local smoothness of the background component on the length scale of the PRF of the solution,  $\mathbf{r}$ .

This research on MCS has been motivated by the specific case of trying to enhance the resolution of low resolution infrared imagery from infrared surveys such as MSX and in the future, similar data that will be available from WISE. For these instruments, the need for a wide field of view drives the plate scale away from that required for true diffraction limited imaging.

## 2. PERFORMANCE LIMITATIONS OF MCS FOR POINT SOURCE SUPER-RESOLUTION

There are a number of limiting factors in performing image super-resolution in general, and with the MCS algorithm in particular. In the general theory, Donoho [4] has showed that the degree to which super-resolution is possible depends on how nearly black the image is. Therefore, it is progressively more difficult to find a super-resolved solution as the number of point sources becomes too high, or if the point sources exist along with structured background that cannot be suppressed for the super-resolution process.

Deconvolution methods also require accurate knowledge of the original point response function at a sampling frequency that allows reconstruction of an image at the desired (higher) resolution. This requires either a well characterized and stable optical system, or an accurate high resolution measurement of the PSF contemporaneously from the imaging system.

The MCS algorithm imposes additional constraints on performance. Firstly, the method is limited in that the degree of super-resolution depends on the new point spread function,  $\mathbf{r}$ , and the fact that the new pixel spacing must be at least Nyquist sampled. Secondly, because the data modeling term models the point sources by a representation of the true system PSF,  $\mathbf{p}$ , deviations from  $\mathbf{p}$  by point sources in the data will introduce errors into the deconvolution results. Deviations in the image data PSF can come from a number of sources, dominated by noise variation. Noise sources can be electronic noise, jitter induced clutter, or Poisson noise.

The ability of MCS to accurately reconstruct both the point source position and amplitude information for point sources will depend (in the noise-free case) on the spatial distance between point sources. Since MCS seeks to reconstruct an image as seen by a superior (i.e. higher resolution) optical system than that of the original data, we expect the reconstruction to break down as the distance between point sources to be resolved approaches the Rayleigh limit for the new system.

In reference [3] I demonstrated that in the noise free case, with perfect knowledge of the low resolution PSF, and having a low resolution image that is oversampled, it is possible to accurately extract the intensity and position of blended point sources that are closer than 0.3 FWHM of the low resolution PSF,  $\mathbf{p}$ , and that very accurate intensity and position information can be extracted up until the point that the sources are unresolved to the new PSF,  $\mathbf{r}$ . For sources within 1 FWHM of  $\mathbf{r}$ , the position and intensity information cannot be determined adequately.

In this paper I investigate the performance of the MCS method for cases more likely to be found in real systems. First, we shall sample the low resolution at the Nyquist frequency defined for the low resolution PSF,  $\mathbf{p}$ , rather than oversampling the low resolution image at the Nyquist rate for the high resolution PSF,  $\mathbf{r}$ . The synthetic low resolution images will be generated from high resolution “truth” images, consisting of 3 point sources – one isolated, and two that will be unresolved to varying degrees in the low resolution images.

The low resolution image will have Gaussian random noise added on a per pixel basis. The variance and amplitude of the noise will be randomly selected per pixel, within prescribed parameters. In some cases, we will examine the effect of jitter on the MCS reconstruction method by producing a set of images in which random x and y offsets are introduced to the “truth” image before it is convolved with the low resolution PSF and down-sampled. The final low resolution image will be formed by co-adding the sets of data that include jitter in order to model the additional point source “blur” introduced by jitter.

Before examining individual effects on the super-resolution performance, I shall baseline the performance of the MCS method for the case where the SNR is  $\sim 100$  in the low resolution image. Here we are increasing the pixel sampling by a factor of 7 pixels between the low resolution and super-resolved images. The FWHM of the associated Gaussian PSFs differ by a factor of 6, 17 high resolution pixels for  $\mathbf{p}$ , and 2.84 high-resolution pixels for  $\mathbf{r}$ . This equates to 2.4 low resolution pixels for the FWHM of  $\mathbf{p}$  and 0.4 low resolution pixels for the FWHM of  $\mathbf{r}$ .

This combination of PSF FWHM and pixel sampling ensures that the sampling theorem is satisfied in the deconvolved super-resolution image.

For ideal optical systems, the classical resolution limit for diffraction limited systems is defined by the Airy criterion,  $1.22\lambda/D$ . This defines the point at which the Airy disk has its first zero. We can also define this limit to be where two point sources are separated by one FWHM of the Airy function, and this is often extended to the non-ideal case where the PSF is not diffraction limited but is a 2-D Gaussian shape. With this criterion, we define sources separated by  $\geq 1$  FWHM as resolved and  $< 1$  FWHM as unresolved.

As test cases we set up point source pairs at the PSF  $\mathbf{p}$  multiples shown in Table 1 and characterized the ability of the MCS algorithm to resolve these sources and accurately extract the source intensity and position information. Table 2 lists the position and intensity values of the point sources, including the isolated source. The high and low resolution images for these cases are shown in Figures 1 through 5.

**Table 1. Parameters of Synthetic Data Point Source Pair**

Case Number	Separation ( $\mathbf{p}$ FWHM)	Separation (low resolution pixels)	Separation ( $\mathbf{r}$ FWHM)	Separation (high resolution pixels)
1	2	4.86	12	34
2	1	2.43	6	17
3	0.5	1.21	3	8.5
4	0.25	0.6	1.5	4.25
5	0.125	0.3	0.75	2.13

In Table 2, source (1) is the isolated source, while sources (2) and (3) are the point source pair that we are trying to resolve in the new image. Table 3 lists the intensity and positions derived from the MCS deconvolution algorithm for each source.

**Table 2. Point Source Parameters - Synthetic Data**

Case #	Source 1 amplitude	Source 1 x coord	Source 1 y coord	Source 2 amplitude	Source 2 x coord	Source 2 y coord	Source 3 amplitude	Source 3 x coord	Source 3 y coord
1	1000	45	140	2000	67	50	1000	57	82.62
2	1000	45	140	2000	67	50	1000	57	63.82
3	1000	45	140	2000	65.5	67	1000	57	67
4	1000	45	140	2000	61.25	67	1000	57	67
5	1000	45	140	2000	59.13	67	1000	57	67



**Figure 1a. Case 1, truth image**

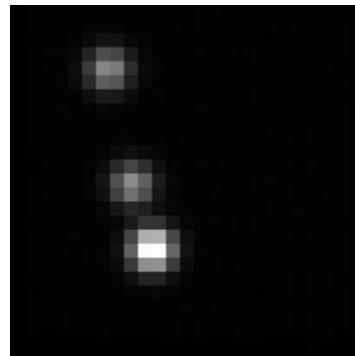


**Figure 1b. Case 1, low resolution**



**Figure 2a. Case 2, truth image**

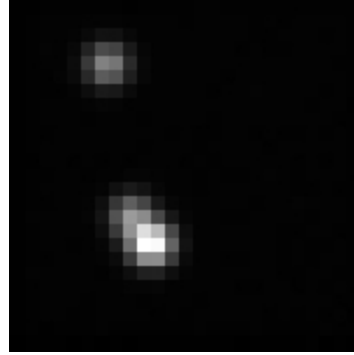


**Figure 2b. Case 2, low resolution**

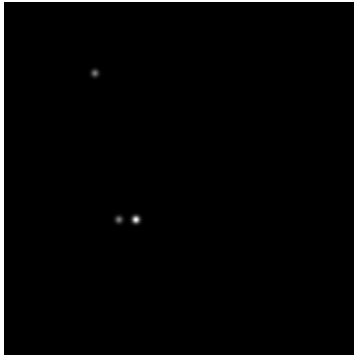


**Figure 3a. Case 3, truth image**

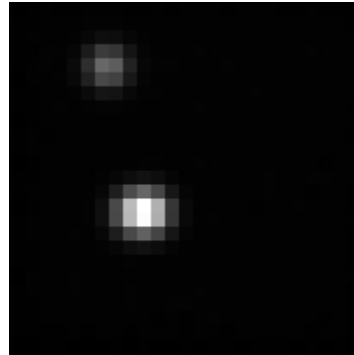


**Figure 3b. Case 3, low resolution**

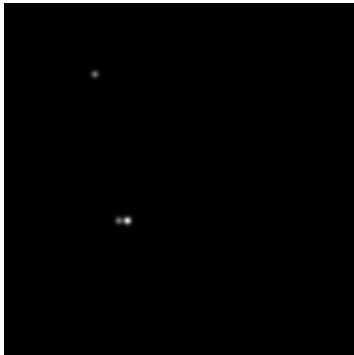


**Figure 4a. Case 4, truth image**

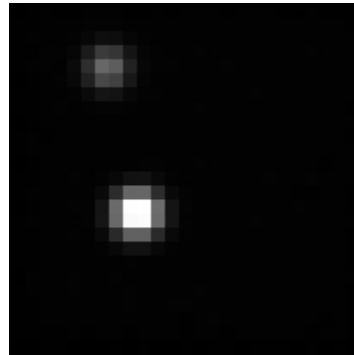


**Figure 4b. Case 4, low resolution**

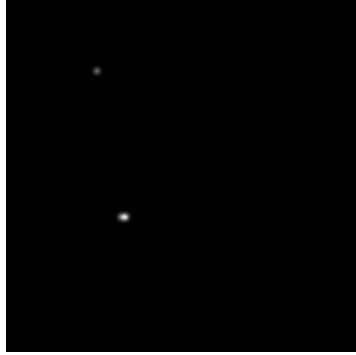


Figure 5a. Case 5, truth image

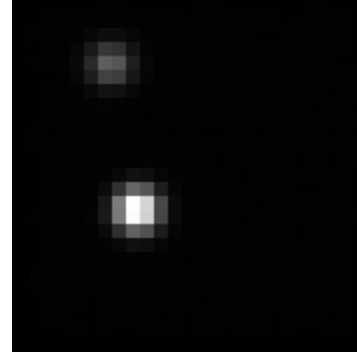


Figure 5b. Case 5, low resolution

Table 3. Point Source Parameters - MCS Results

Case #	Source 1 amplitude	Source 1 x coord	Source 1 y coord	Source 2 amplitude	Source 2 x coord	Source 2 y coord	Source 3 amplitude	Source 3 x coord	Source 3 y coord
1	1042.3	44.67	139.78	1999.5	66.7	49.7	1034.6	56.6	82.5
2	1038.0	44.69	139.81	1606.1	67.4	48.3	1289.9	58.8	59.5
3	995.9	44.33	141.38	1529.2	65.8	66.4	1390.2	59.1	66.8
4	993.12	44.66	139.77	1499.1	61.1	66.4	1497.0	58.0	67.0
5	927.9	45	140	1484.3	58.1	66.7	1454.3	58.1	66.7

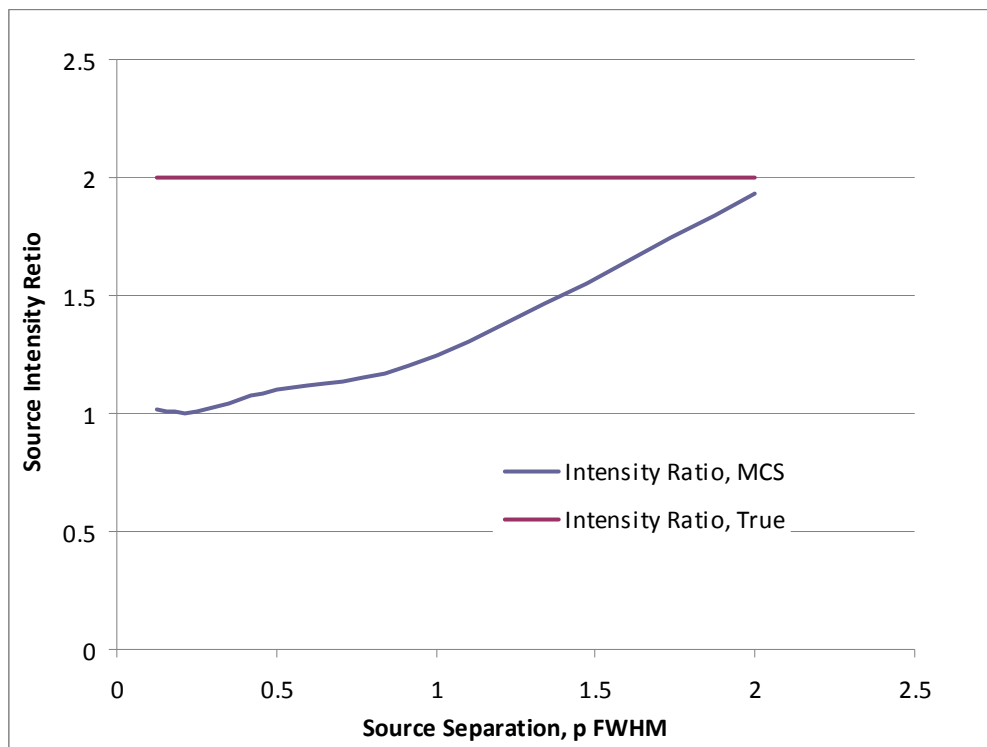
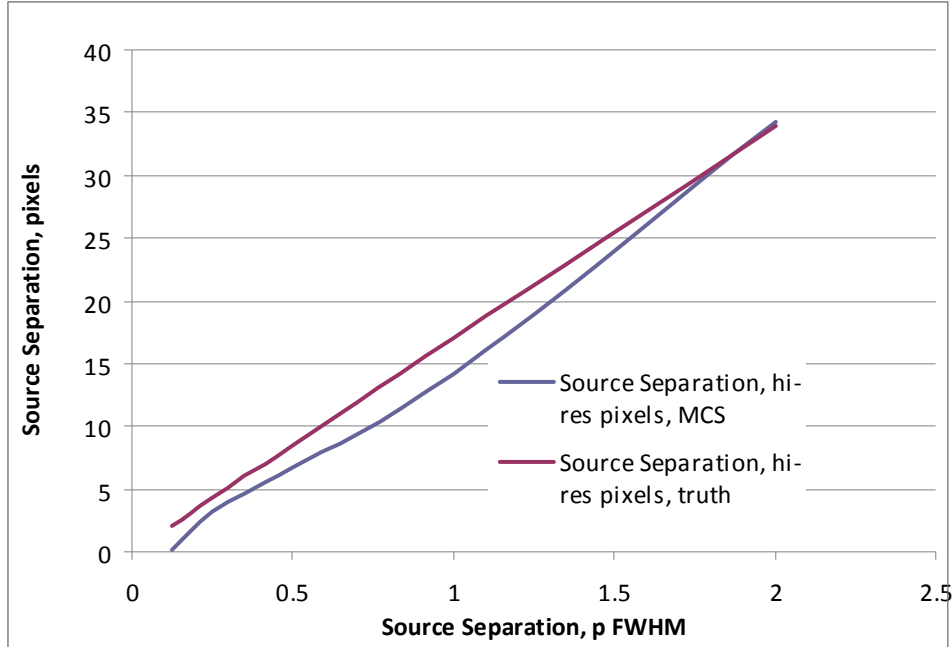


Figure 6. Source Intensity Ratio as a function of source separation



**Figure 7. Deconvolved Source Separation as a function of true source separation**

Figures 6 and 7 show the results of the MCS deconvolution for the point source pair as a function of separation distance expressed in terms of low resolution PSF FWHM. As the point sources become unresolved in the low resolution image, it becomes more difficult for the algorithm to recover the correct point source amplitude, and the algorithm tends to divide the total flux equally between the two point sources, even though in this case one source is twice as bright as the other. The algorithm performs better in terms of determining accurate point source positions, at least while the point sources are separated by greater than one FWHM of the new system PSF,  $\mathbf{r}$ .

### 3. EFFECT OF PSF KNOWLEDGE ON SUPER-RESOLUTION

The above super-resolution examples have been computed using the analytic form of the PSF,  $\mathbf{p}$ , sampled onto the high resolution grid – in other words, we have assumed essentially perfect knowledge of the system characteristics of the low resolution system. In practice, we rarely know this – there are focus issues in real systems due to environmental and other issues that preclude perfect knowledge of the system. In these cases, we must measure the PSF in real time, generally by using a known isolated point source to construct a PSF.

In our case, we shall use the isolated point source in the test data to reconstruct a point spread function. We will use the “jittered” images described in section 2, and the technique of variable linear pixel reconstruction (or “drizzle” to construct point spread functions at a variety of sampling resolutions, ranging from 100 samples per low resolution pixel, down to a one-to-one PSF sampling of the low resolution data.

We then use each sampled PSF as the “ $\mathbf{p}$ ” operator in the MCS algorithm, and examine the degree to which the correct point source separation is recovered by the algorithm. The case where SNR is  $\sim 100$  is used in order to isolate the effects of point source sampling. The true source separation is the case where the point source pair is separated by 0.75 FWHM of  $\mathbf{p}$ . This is a separation of 1.8 low resolution image pixels or 12.75 hi resolution image pixels. The results are shown in Figure 8.

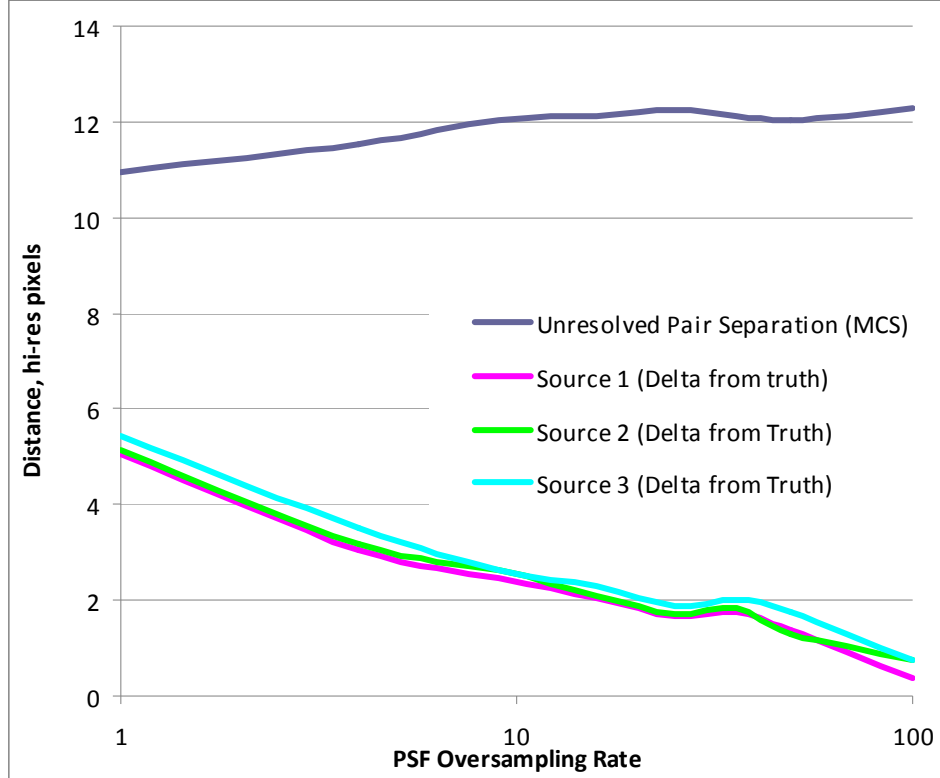


**Figure 8. MCS Separation as a function of PSF Knowledge**

As the the sampling rate declines, the performance is degraded for both absolute point source position knowledge and the ability to accurately find the separation between unresolved point sources. The primary effect of PSF sampling knowledge appears to be on absolute position extraction, The deviation from truth with PSF oversampling rate is about the same for the isolated source and the unresolved point source pair, ranging from less than one high resolution pixel for the highly oversampled PSF, to a deviation of 5 high resolution pixels ( $\sim 0.7$  low resolution pixel) for the case where the PSF is only sampled at the original low resolution image sampling rate. The effect on the MCS extracted source separation was less pronounced, with the unresolved point sources pair separation being reported to be slightly less as the PSF is progressively more undersampled. Still, even with the lowest resolution PSF used for the MCS reconstruction, the reported separation distance is better than 85% of the true separation distance.

#### 4. SNR AND SUPER-RESOLUTION PERFORMANCE

Based on previous work, we expect that the signal to noise ratio is a strong limiting factor on the ability to perform super-resolution deconvolution. The addition of noise will degrade the ability of the MCS method to find an accurate fit to the data. As noise increases, the amount of information that is characteristic of the PSF in the image decreases. This degradation appears first in the wings of the PSF, and erodes into the core of the PSF as the SNR decreases. In Fourier space, this implies that the amount of usable frequency information is reduced as SNR decreases. Therefore we expect that the degree to which we can accurately reconstruct a super-resolved image will decline with SNR.

Again we use the case where the source separation of 0.75 FWHM of the low resolution PSF. We shall use the analytic form of the PSF,  $\mathbf{p}$  in order to isolate the effects of SNR. Figure 9 demonstrates that our expectations hold – the calculated separation is accurate for the MCS method in the high SNR cases. As the SNR drops below  $\sim 30$ , however, we start to see degraded performance, specifically a decrease in the computed separation distance. This is

consistent with the loss of high frequency information that results in the ability of the method to distinguish the presence of multiple point sources. By a SNR of 5 the method reports both sources in the unresolved pair at virtually the same point. The increase in noise also introduces error into the extracted position of the isolated source, and this error increases as the SNR decreases. Note that the isolated source has a lower SNR by a factor of two than the point source pair for each image.

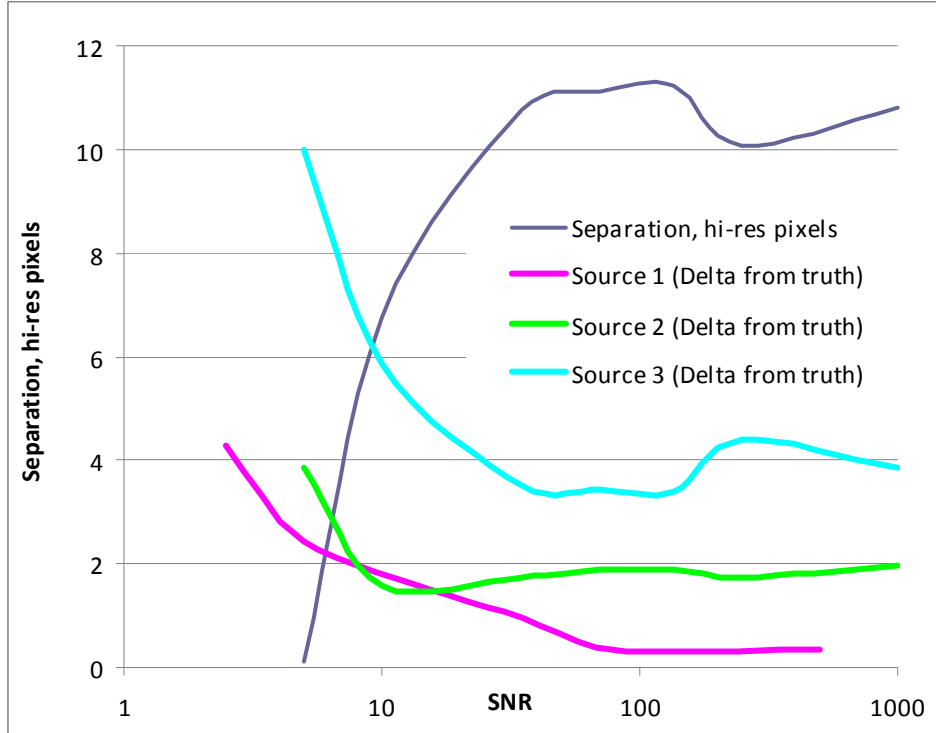


Figure 9. MCS Separation as a function of SNR

## 5. JITTER INDUCED DEGRADATION OF SUPER-RESOLUTION PERFORMANCE

As described in Section 2, jitter could be introduced to the system, and co-added final low-resolution images constructed that mimic images produced under conditions of sensor jitter. The effect of sensor jitter is two-fold, in that it will change the noise character of the image, and it essentially alters the point spread function in the low resolution image by broadening the PSF,  $\mathbf{p}$ , beyond the true FWHM of the optical system. Therefore inaccuracies will be introduced in the data modeling term of the MCS equation.

In order to quantify the effect of this broadening on the results of MCS super-resolution method, we again examine the SNR  $\sim 100$  case with point sources separated by 0.75 FWHM of the low resolution system. We examine cases beginning with no jitter, and increase the mean jitter amplitude by steps of 0.2 low resolution pixels, up to a maximum of 1.4 low resolution pixel of jitter. Results are displayed in Figure 10, and show that performance is degraded as a function of image jitter. While the separation distance found for the unresolved sources is not strongly affected, the absolute position values are. The absolute position error is directly correlated to the number of co-added frames used to make the low resolution image and the amount of jitter. The co-addition introduces a random walk error into the positions, and as expected, the extraction error for source positions is approximately equal to  $N^{1/2}A_j/2$ , where  $N$  is the number of frames co-added and  $A_j$  is the jitter amplitude.



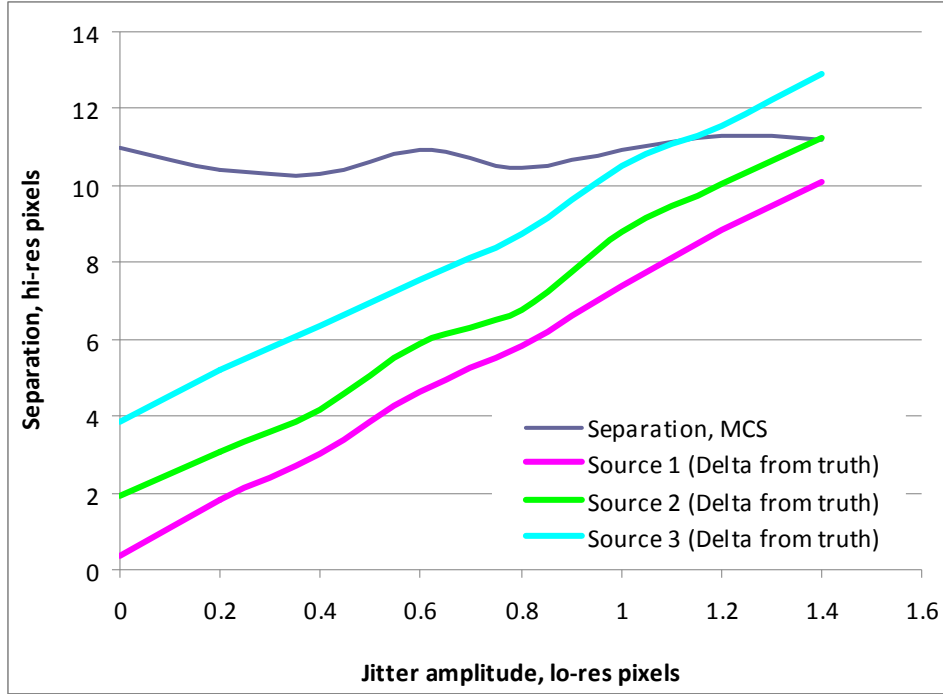


**Figure 10. MCS Separation as a function of jitter amplitude**

## 6. CONCLUSIONS

In cases representative of real systems, we have quantified the performance limitations of the MCS super-resolution algorithm. Noise sources that impact the degree of accurate knowledge of the original system PSF, including low SNR, system jitter, and poor PSF measurement or reconstruction will negatively impact the ability to accurately model the true image parameters and result in poor position information being returned for the point sources. We have also examined the overall algorithm limitations, and find that although the method does yield accurate position information, given good PSF knowledge and adequate SNR for sources that would be resolved by the high resolution system being modeled by the MCS method, the amplitudes of the point sources tend to be averaged together as the source separation decreases.

## REFERENCES

1. Magain, P., Courbin, F., Sohy, S., Deconvolution with Correct Sampling, *The Astrophysical Journal*, Vol. 494, 472-477, 1998.
2. Egan, M., Testing the MCS Deconvolution Algorithm on Infrared Data, *AMOS Conference Proceedings*, 2007.
3. Egan, M, The super-resolution of linear structures in image data, *AMOS Conference Proceedings*, 2008.
4. Donoho at el., *Journal of the Royal Statistical Society*, Vol. 54, 41, 1992.